ELSEVIER

Chemical Engineering Journal 125 (2006) 1–8

Chemical Engineering Journal

www.elsevier.com/locate/cej

Jet configuration for improved fluidized bed stripping

Heping Cui [a], John Grace [a,*], Craig McKnight [b], Tianzhu Zhang [a], Ian Rose [b], Xiaotao Bi [a], Jim Lim [a], Darren Burgardt [b]

[a] *Department of Chemical and Biological Engineering, University of British Columbia, Vancouver, Canada V6T 1Z3*
[b] *Syncrude Research, 9421-17 Avenue, Edmonton, Alta., Canada T6N 1H4*

Received 2 April 2005; received in revised form 4 February 2006; accepted 21 February 2006

Abstract

The effects of steam injection on stripping efficiency were studied in an effort to improve operation of a fluidized bed stripper. Experiments extend earlier measurements in a geometrically and dynamically scaled half-column [I. Rose, H. Cui, T. Zhang, C. McKnight, J.R. Grace, X.T. Bi, C.J. Lim, Toward an ultimate fluidized stripper, Powder Technol. 158 (1–3) (2005) 124–132]. In the present work, different jet/steam configurations were tested in a stripper equipped with mega-sheds, in an effort to greatly reduce stripper fouling while providing little or no reduction in stripping efficiency. Results indicate that a combination of spargers, jets sweeping across the top of the sheds and additional staggered jets provides a promising configuration, giving stripping efficiencies similar to those of the original commercial design while being much more tolerant to accumulation of foulant.

Keywords: Fluidized bed; Fluid coker; Stripping efficiency; Jets; Gas–solid flow

1. Introduction

Gas–solid strippers are widely used in fluid catalytic cracking (FCC) units [2,3] and fluid cokers [4] to strip residual liquid hydrocarbons from the surface of underflow solid particles, and to prevent underflow of hydrocarbon gases. In both applications, an assembly of horizontal or inclined baffles is employed to increase gas–solid contacting, prevent particle short-circuiting, reduce gas bypassing via large bubbles, improve the radial distribution of gas, and reduce axial dispersion, thereby increasing stripping efficiency.

Fluid cokers are large fluidized bed reactors used for thermal cracking of heavy hydrocarbon molecules into distillate products. Hot solid particles, introduced from above, provide the heat required for the endothermic cracking reactions and collect solid by-products on their surfaces. Hydrocarbon feed is injected through rows of horizontal nozzles in the upper part (feed section) of the reactor. Vaporized products rise through the bed, counter-current to coke particles, which descend to the lower "stripper" section in which steam removes surface liquid and interstitial hydrocarbon gases. This stripping, combined with additional solids residence time to further react any residual surface liquid, minimizes carry-under of hydrocarbon product to the burner. Fluid cokers operate close to the bubbling–turbulent fluidization transition velocity, with net upflow of the gas and counter-current net downflow of the solid particles [5–7]. After passing through the stripper and transfer via a standpipe, the coke particles are circulated to a separate fluidized bed burner for re-heating, prior to re-entering the fluid coker at an increased temperature to supply heat to the fluid coker.

Fouling of the top rows of stripper baffles and of the standpipe entrance is a major and persistent issue for commercial fluid cokers, leading to flooding [8], reduced run length, time-consuming and expensive cleanup during shutdowns, and operational constraints. Some success has been achieved in reducing fouling in recent years by modifying commercial strippers based on findings [6] from the same geometrically and dynamically scaled cold model unit as was used in this paper.

Further steps are needed for the commercial strippers to ensure reliable and aggressive runs of longer duration without interruptions due to fouling, flooding and standpipe entrance reversals, while maintaining, or even increasing, throughputs. Hence work was undertaken in search of an improved stripper that would accomplish these objectives. Various stripper

* Corresponding author. Tel.: +1 604 822 3121; fax: +1 604 822 6003.
E-mail address: jgrace@chml.ubc.ca (J. Grace).

1385-8947/$ – see front matter © 2006 Elsevier B.V. All rights reserved.
doi:10.1016/j.cej.2006.02.016

Nomenclature

d_o	inside diameter of nozzle (m)
d_p	average diameter of bed particles (m)
g	acceleration of gravity (m/s^2)
L_{ave}	average jet penetration length (m)
m_s	solids circulation rate (kg/s)
P	pressure at nozzle tip (Pa)
$Q_{He\text{-}stp}$	flow rate of helium down the standpipe (m^3/s)
$Q_{He\text{-}tot}$	total flow of helium injected through feed nozzles (m^3/s)
Q	total gas carry-under into standpipe (m^3/s)
Q'_0	total gas flow introduced into stripper/Q_{sc} (−)
Q'_{bn}	air flow rate of bottom nozzles/Q_{sc} (−)
Q_{sc}	representative industrial stripper gas flow rate (m^3/s)
Q'_{st}	total air flow of jets and spargers in stripper (above standpipe entrance)/Q_{sc} (−)
T	temperature (°C)
u_0	jet velocity at nozzle tip (m/s)
U'_g	superficial gas velocity/typical industrial stripper superficial velocity(−)
ε	bed voidage (−)
ρ_0	density of jet at nozzle tip (kg/m^3)
ρ_f	density of fluidizing gas (kg/m^3)
ρ_p	particle density (kg/m^3)
$\eta_{stripper}$	stripping efficiency (%)

configurations were tested and evaluated in an effort to find a configuration with a stripping efficiency comparable to the original commercial stripper design, without requiring more steam, but with significantly enhanced tolerance to fouling. The most promising configuration that maximized open area while maintaining stripping efficiency was found to consist of two pairs of large perpendicular crossed horizontal-sheds (intersecting at the axis of the column), with the sheds of the upper pair rotated by 45° relative to those of the pair below. This geometry, combined with horizontal, parallel jets, gave stripping efficiencies close to the commercial fluidized bed stripper design [1], showing potential for future development and commercialization. This paper focuses on exploration of optimal stripping steam configurations to achieve the most promising stripping efficiency, without introducing more stripping steam. In addition, it explores steam injection configurations which could reduce attrition.

2. Experimental

2.1. Equipment and operating conditions

A schematic of the semi-circular Plexiglas geometrically scaled fluid coker cold flow model appears in Fig. 1. All dimensions were approximately an order of magnitude smaller than the corresponding dimensions of Syncrude's two fluid cokers. Dynamic similarity was achieved in the stripper section by matching all important dimensionless groups, based on dimensional analysis [9]. This meant that the bed operated near the transition between bubbling and turbulent fluidization.

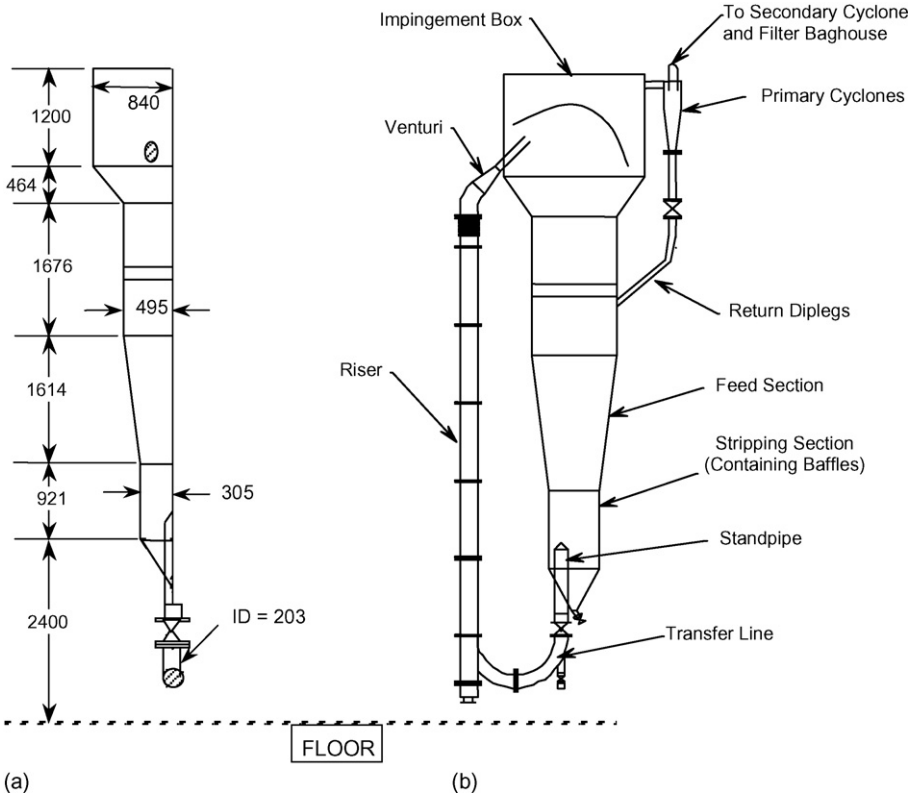

Fig. 1. Overall schematic of semi-circular cold model fluid coker: (a) side view; (b) front view (all dimensions are in millimeters).

The riser had a diameter of 0.2 m, while the stripper was 0.61 m in diameter. FCC particles of mean diameter 97 μm and density 1700 kg/m^3, with fines removed to improve the matching of the particle size distribution, were used in the experiments. Pressurized air was introduced through numerous nozzles and spargers located in the stripping and feed sections. For the base case experiments, the gas flow distribution was set such that each nozzle contributed the same fraction of the overall flow as its counterpart in Syncrude's two commercial fluid cokers and such that the jet penetrated the same fraction of the column radius. The jet penetration was estimated based on the correlation of Merry [10] which had been shown to give good predictions of horizontal length in our previous study in the same column with the same particles. With the unit operating under steady state conditions, the net flow of particles was downward through the reactor section and stripper. Solids left the column through a standpipe conical entrance whose vertex was located asymmetrically just below the bottom row of stripper baffles of the original commercial design, with the overall solids circulation rate controlled by a pinch valve in the standpipe. The solids were then carried pneumatically through a J-valve and vertically upward through a riser. As they left the top of the riser, they passed through a venturi constriction and impinged on a curved separation baffle, acting as a low-pressure-drop gas–solid separator, which removed most entrained particles, facilitating their return to the top of the dense bed in the coker unit. Air from both the riser and the main reactor, as well as entrained particles, passed through six primary parallel cyclones after leaving the top of the model coker. Particles separated by these cyclones were returned through diplegs to the dense bed below its free surface. A secondary cyclone and two parallel bag filter houses captured any remaining particles before the off-gases were vented to the atmosphere.

The solids circulation rate through the system was determined from the pressure drop across the venturi constriction at the top of the riser after calibration by concurrently measuring the steady state solids circulation rate in the standpipe using a fibre optical probe [11] to simultaneously determine the solids concentration and velocity under steady state operating conditions.

2.2. Stripper configurations

2.2.1. Original commercial design

The original commercial stripper section was equipped with eight staggered rows of "sheds" (90° included top angle) as shown in Fig. 2 [1,6], with a minimum total open area of 50%. The vertical distance from the bottom of one row to the top of the next row below was 50 mm. A row of 11 attrition nozzles, each directed radially inward, was located at the bottom of the feed section (reactor). Several spargers, with a dimensionless total flow rate of 0.003 (total flow rate divided by the typical industrial stripper gas flow rate), were installed under the lowest two rows of sheds to uniformly introduce the air (simulating steam in the commercial units). In addition, two rows of stripping nozzles were located at the bottom of the stripper, providing a dimensionless total air flow rate of $Q'_{bn} = 0.002$. The bottom stripping nozzles were maintained for all new configurations investigated below. More information on the stripper geometry and sheds is

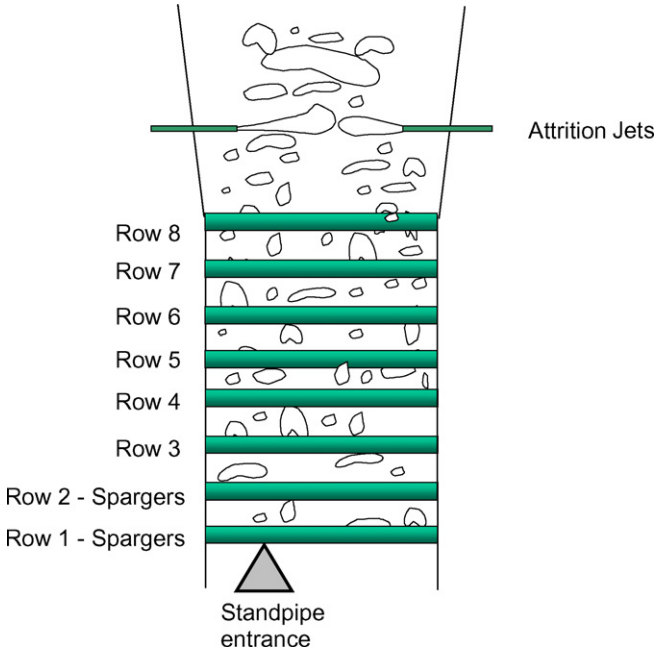

Fig. 2. Configuration of original commercial stripper section. All eight rows of sheds have 90° top-included-angle (all dimensions are in millimeters) [1,6].

provided by Bi et al. [6]. The solids circulation rate varied from 6.7 to ~11 kg/s, while the dimensionless superficial gas velocity was maintained at $U'_g = 0.75$ at the top of the stripper.

2.2.2. Mega-sheds combined with 18 horizontal jets

As reported previously [1], a newly developed ultimate fluidized bed stripper with two mega-sheds could achieve a stripping efficiency similar to those with three mega-sheds and three wall baffles, or three mega-sheds. The wall baffles contributed little and can likely be omitted to simplify the internals design. The mega-sheds consisted of two inverted-V's meeting at right angles, each with a slope of 45° to the horizontal. In plan view, these were either like the upper half of a plus sign (+) or the upper half of an X in the half-column (see Fig. 3). For ease of reference, they are referred to here as the "+-mega-shed" and "X-mega-shed", respectively. Both were designed

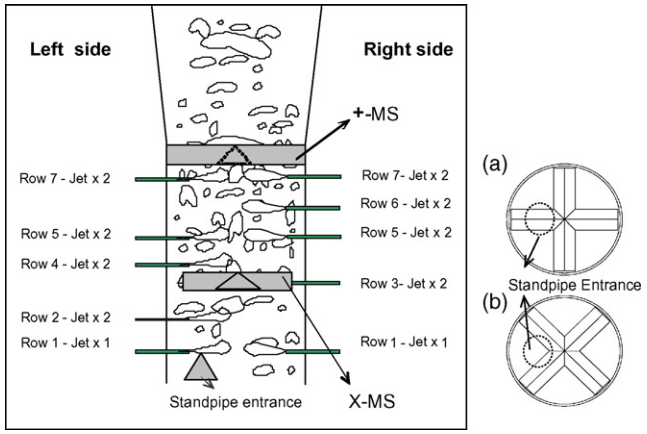

Fig. 3. Stripper configuration with 18 horizontal wall jets and two mega-sheds: (a) +-configuration, (b) X-configuration.

Table 1
Configurations of spargers and jets tested with three spargers under the bottom +-mega-shed

Case	Active jets, left side	Active jets, right side	Jets staggered?	Spargers	Q'_{st}
1	0	0	N.A.	0	0
2	0	0	N.A.	3	0.0045
3	0	0	N.A.	3	0.0031
4	2 in row 2, 2 in row 4, 2 in row 7	2 in row 4, 2 in row 6, 2 in row 7	Most	3	0.0061
5	2 in row 2, 2 in row 4, 2 in row 6	2 in row 2, 2 in row 5, 2 in row 6	Partial	3	0.0061
6	1 in row 1, 2 in row 2, 2 in row 4, 1 in row 6	1 in row 1, 2 in row 2, 2 in row 5, 1 in row 6	Partial	3	0.0061
7	1 in row 1, 2 in row 2, 2 in row 4	1 in row 1, 2 in row 2, 2 in row 5	Partial	3	0.0051

N.A. = not applicable.

to provide minimum open areas of 50% of the column cross-section, as for each row of sheds in the original commercial design.

In the work summarized in this paper, the two mega-shed configurations were further tested in combination with various steam injection geometries in a search for an optimal stripping steam configuration for the ultimate fluidized bed stripper. One mega-shed was fixed at the top of the stripper and the other was 370 mm lower. Two options, "+-top, X-bottom" and "X-top, +-bottom", were tested to determine whether stripping efficiency depends on the placement of the mega-sheds relative to the exit standpipe. The "+-top, X-bottom" represents the configuration of a +-mega-shed on the top and a X-mega-shed at the bottom, as shown in Fig. 3. The attrition nozzles at the bottom of the feed section were removed for these tests and the incoming air (simulating steam) was re-distributed.

The tests were first carried out with 18 parallel jets in the stripper and a dimensionless total air flow rate of $Q'_{st} = 0.0092$. This configuration had been found in early screening to have potential to achieve high stripping efficiencies without requiring extra steam compared to the total steam from attrition nozzles and spargers in the original commercial design. There were 18 horizontal nozzles of diameter 6.4 mm arranged in seven rows (levels) as shown in Fig. 3. The dimensionless superficial gas velocity was 1.64 at the top of the stripper. The air flows to each nozzle were very nearly equal because the pressure drop over the line connecting the nozzle to a common header was much larger than the difference of hydrostatic pressure on the fluidized bed side. Two nozzle insertions were tested, one with 18 jets flush with the wall, the other with 12 jets flush with the wall and six inserted 90 mm from the wall (four in row 7, and two in row 3) to investigate the effect of jet insertion.

2.2.3. Mega-sheds combined with spargers and free jets

To explore the possible application of spargers, three spargers were installed beneath the bottom mega-shed (+) for some tests ("X-top, +-bottom" configurations), replacing six of eighteen jets, as shown in Fig. 4. The dimensionless total steam flow from the spargers was normally 0.0031, half of that for the 12 jets. The dimensionless superficial gas velocity was 1.64 at the top of the stripper.

Different jet configurations combined with spargers were then tested to clarify the influence of the location and number of jets. All nozzles were flush with the inner wall. The configurations and conditions tested are listed in Table 1.

2.2.4. Mega-sheds combined with spargers and sweeping jets as well as free jets

We further explored whether horizontal sweeping jets, along the top of the sheds can reduce the possibility of shed fouling, while contributing to high stripping efficiency. As shown in Fig. 5, two spargers were installed beneath the bottom shed for the +-top, X-bottom configuration. These two spargers had the same total dimensionless air flow rate (0.0031) as the six jets. Five jets swept the tops of both mega-sheds, one along each radius in the half-column. Seven staggered free jets were located near the bottom of the stripper, referring to the preliminary optimization of jets (left side: two in row 2, and two in row 5; right side: one in row 1, two in row 3). The total air flow rate of the two spargers, five sweeping jets and seven free jets was the same as for the 18 parallel jets described above, with the dimensionless superficial gas velocity again 1.64 at the top of the stripper.

To study how spargers and jets separately influence the stripping efficiency, several configurations were tested with the +-top, X-bottom configuration: (a) no spargers, no jets; (b) two spargers, no jets; (c) two spargers, five sweeping jets; (d) two spargers, five sweeping jets and seven free jets.

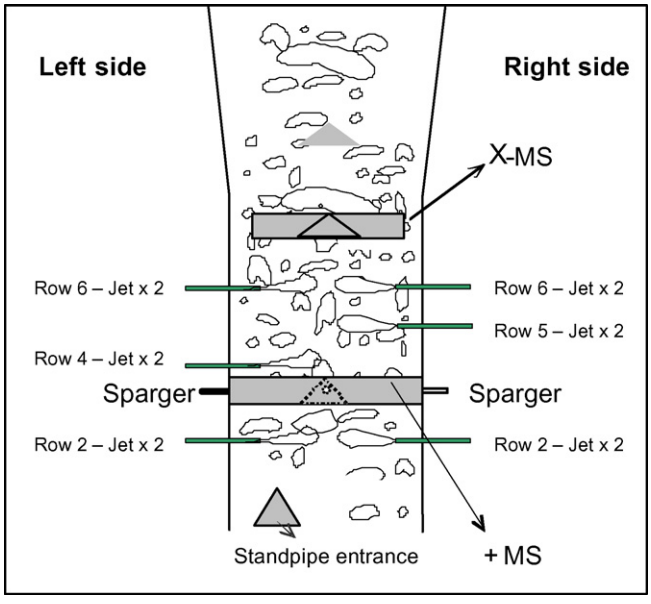

Fig. 4. Stripper configuration with two mega-sheds and 12 horizontal wall jets as well as three spargers beneath bottom + mega-shed (Case 5 Table 1).

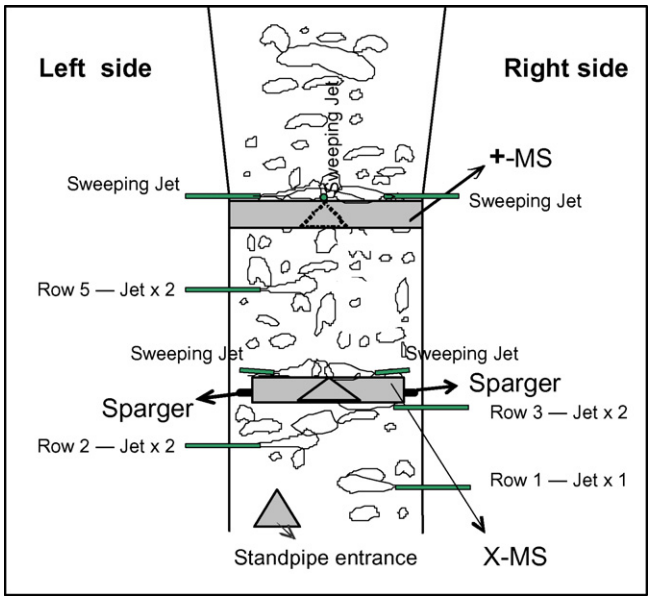

Fig. 5. Stripper configuration with two mega-sheds ("+-top, X-bottom" configuration), two spargers beneath X-bottom mega-shed, five sweeping jets on top of two mega-sheds, and seven free jets (left side: two in row 2, and two in row 5; right side: one in row 1, two in row 3).

2.2.5. Mega-shed with large-diameter nozzle jets

During the screening work with 18 jets and no internals in the stripper, it was found that 18 small completely open nozzles of diameter 3.2 mm with a dimensionless flow rate up to 0.0072 (the maximum allowed by the available air pressure) could reach stripping efficiencies as high as those of the 18 normal nozzles with a dimensionless total flow rate of 0.0093. If the flow rate of normally scaled (6.4 mm diameter) nozzles was decreased to the maximum flow rate of the smaller nozzles, the stripping efficiencies decreased. This suggests that smaller nozzles achieve a higher stripping efficiency for the same steam flow rate, presumably because the penetration of the jet is greater. However, the small nozzles were unable to introduce enough air (simulating steam) for the stripping process with the available pressure.

To investigate further how the jet nozzle diameter affects the stripping efficiency, twelve 9.5 mm diameter nozzles (henceforth called "large nozzles") were installed, replacing the twelve 6.4 mm jet "normal" nozzles. Five of these large nozzles served as sweeping jets, while seven were free jets. Each large nozzle had the same air flow rate as the normal nozzles. The +-top, X-bottom configuration with large jet nozzles was tested for the same operating conditions as described in the previous subsection (Fig. 5).

2.3. Measurement system

The injection system introduced helium tracer at constant and equal flow rates through the bottom feed nozzles to simulate feed hydrocarbon injection into the commercial reactors. The general experimental set-up for the tracer studies was the same as described by Rose et al. [1] and Cui et al. [12].

The gas-sampling probe was located in the standpipe below the stripper, consisting of a 6.4 mm diameter tube with a 15 μm sintered metal filter tip, leading to a thermal conductivity detector (TCD). The TCD signal passed through an amplifier into a calibrated data acquisition system. LABTECH Notebook software recorded the TCD signal at a sampling frequency of 5–10 Hz and also triggered a solenoid valve. A needle valve situated upstream of the detector dampened signal fluctuations.

The helium concentration in the standpipe detected by the TCD sampling system allows the entrainment of hydrocarbon into the standpipe to be estimated, thereby providing an estimate of stripping efficiency [12]. Helium is a non-adsorbing tracer and the FCC particles are porous, whereas some hydrocarbon is carried on the outer surface of the non-porous coke particles in the real system. Hence the stripping efficiencies determined in the cold model are unlikely to provide accurate quantitative measurement of stripping efficiency in the commercial system, but they should provide an excellent indication of the influence of operating conditions and of the relative merits of different configurations. All tests and measurements were repeated for each condition to provide a measure of reproducibility.

3. Results and discussion

3.1. Stripper efficiency

Tests were carried out to obtain axial tracer concentration profiles in the stripper with helium injected steadily through bottom feed nozzles into the reactor. The aim was to determine how much tracer descended through the standpipe, and hence to estimate the "stripper efficiency". Pronounced local gradients and fluctuations in tracer gas concentration made it impossible to determine accurate local efficiencies. Consistent and meaningful results were instead obtained by determining an overall "stripping efficiency" based on helium detected across the standpipe from

$$\eta_{\text{stripper}} = 1 - \frac{Q_{\text{He-stp}}}{Q_{\text{He-tot}}} \quad (1)$$

where $Q_{\text{He-tot}}$ is the total flow rate of helium injected through the feed nozzles and $Q_{\text{He-stp}}$ is the time-mean and cross-sectionally averaged flow of helium down the standpipe. The latter was obtained as detailed elsewhere [12].

By analyzing data from repeated runs, it was found that the average standard deviation of stripping efficiency was less than 0.01% for all tests. Thus, differences between each configuration in our study were significant from a statistical point of view.

3.2. Stripper with 18 parallel jets

As shown in Fig. 6, a stripper with two mega-sheds, combined with an optimal configuration of 18 parallel jets, can achieve stripping efficiencies approaching those of the commercial stripper. The stripping efficiencies for the +-top, X-bottom configuration appeared to be higher than those of the X-top and +-bottom, with the difference probably due to changes in gas–solids flow near the standpipe entrance.

Insertion of the six jet nozzles (90 mm from the wall) did not have an observable adverse effect on the stripping efficiency for

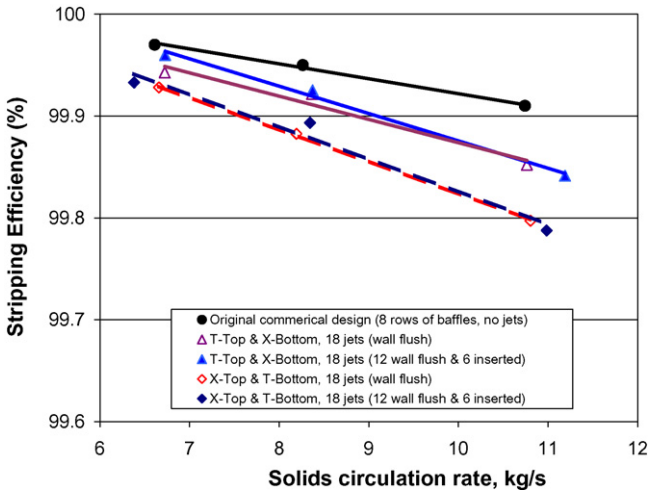

Fig. 6. Stripping efficiencies for five configurations at different solids circulation rates, all with 18 jets and dimensionless air flow rate = 0.0092.

either mega-shed geometry. All configurations with six inserted jets plus 12 wall-flush jets resulted in stripping efficiencies similar to those for 18 wall-flush jets. Thus, insertion of steam nozzles, employed in the commercial units to prevent blockage of nozzles due to build-up of wall coke, did not lead to decreased stripping efficiency.

3.3. Mega-sheds combined with spargers and parallel jets

Fig. 7 compares the results for various configurations of jets combined with spargers for the X-top, +-bottom mega-shed combination with those for the original commercial design and the 18-jet configuration. The stripping efficiency was relatively low at a solids circulation rate of 6.7 kg/s, with no stripping gas introduced from either spargers or jets. When spargers were turned on with a constant dimensionless air flow rate of 0.0031, and with no jets, the stripping efficiency still appeared to be low. The stripping efficiency tended to increase with increasing airflow from the spargers. A combination of three spargers and 12 parallel jets (Case 4 in Table 1: all wall-flush, with two each in rows 2, 4 and 7 on the left side, and two each in rows 4, 6 and 7 on the right side) achieved stripping efficiencies similar to those for the 18 parallel jets, when combined with mega-sheds. This suggests that it is possible to replace some jets with spargers, e.g. to reduce particle attrition during start-up and shutdown.

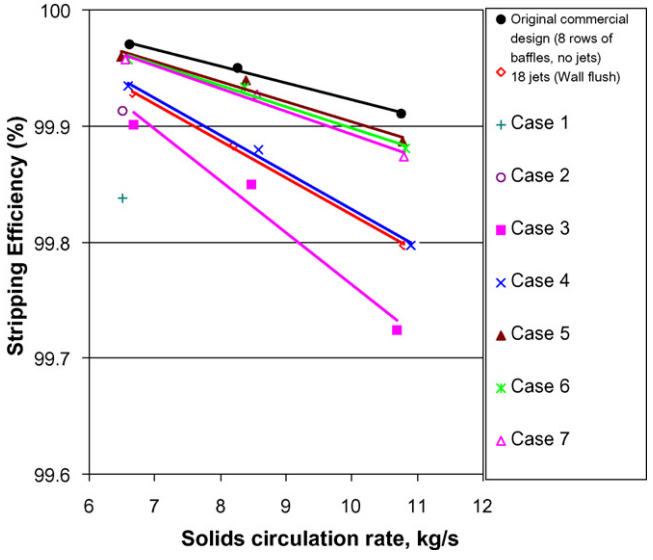

Fig. 7. Stripping efficiencies for various configurations of jets and spargers with mega-sheds (X-top, +-bottom), compared with 18 jets and original commercial design. See Table 1 for configurations and flows for the seven cases.

As shown in Fig. 7, a staggered arrangement of jets from six rows (no jets in row 7) led to higher stripping efficiencies at various solid circulation rates (Cases 5, 6 and 7 in Table 1), close to those of the original commercial design. All three of these promising configurations had jets below the top mega-shed. The existence of a dilute region under the top sheds may have contributed to the high stripping efficiencies, preventing hydrocarbon from being dragged downward by particles descending to the standpipe. The dilute region under the top shed may behave like a flooded region [8]. A combination of three spargers with 12 (or even 10) jets can achieve high stripping efficiencies. Fig. 4 indicates that even the worst configuration with three spargers and 12 jets (Case 4 in Table 1) examined in this study, did not show a large decrease in stripping efficiency. This indicates that two-mega-shed configurations tested, combined with spargers and jets, have good potential to combine favourable stripping efficiency with the ability to tolerate substantially more fouling and reduce flooding.

3.4. Mega-sheds combined with spargers and sweeping/parallel jets

As seen in Fig. 8, a configuration which combined sweeping jets with spargers and parallel jets achieved the highest stripping efficiencies of all mega-shed geometries tested. A combination of five sweeping jets and seven free jets gave stripping efficiencies similar to those of the best arrangement of 12 parallel jets (for example, two each in rows 2, 4 and 6 (left side), and also in

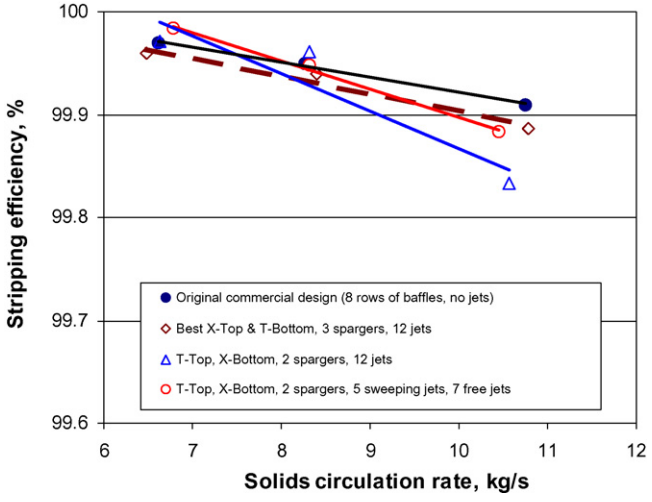

Fig. 8. Stripping efficiencies for two spargers, five sweeping jets and seven free jets compared with other configurations (dimensionless air flow rate = 0.0092).

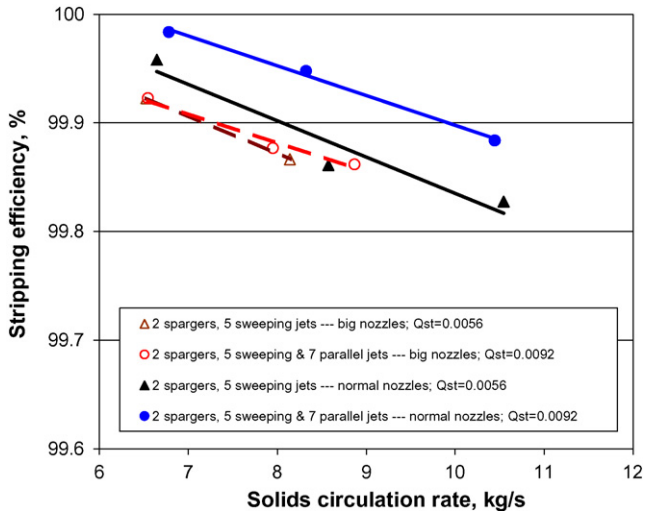

Fig. 9. Stripping efficiency for different enlarged nozzles (9.5 mm diameter) and normal (6.4 mm diameter) nozzles with +-top, X-bottom mega-shed configuration.

rows 2, 5 and 6 (right side) with +-Top, X-bottom configuration. Thus sweeping jets cannot only clean and protect mega-sheds, but they can also give favourable stripping efficiencies. A combination of spargers, sweeping jets and free jets appears to be beneficial.

3.5. *Effect of nozzle diameter on stripping efficiency*

The jet configurations with enlarged nozzles (9.5 mm) caused a relatively high helium concentration in the standpipe, resulting in reduced stripping efficiencies compared with the normal nozzles, as shown in Fig. 9. When the larger nozzles were used, the configuration with two spargers + five sweeping jets + seven parallel jets behaved even worse than the configuration of two spargers + five sweeping jets, with nozzles of normal size. The likely reason is that the jet penetration was reduced for the larger nozzles at the same steam flow rate. The jet penetration length, L_{ave}, predicted by the correlation of Merry [10]:

$$\frac{L_{ave}}{d_0} + 4.5 = 5.25\left[\frac{\rho_0 u_0^2}{(1-\varepsilon)\rho_p g d_p}\right]^{0.4}\left(\frac{\rho_f}{\rho_p}\right)^{0.2}\left(\frac{d_p}{d_0}\right)^{0.2} \quad (2)$$

decreased to 0.16 from 0.25 m when the nozzles of normal size were replaced by the larger ones, as shown in Table 2. The predicted jet penetration length was only about one-quarter of the column diameter for the large nozzles, too little to uniformly dilute the gas–solid flow over the entire column cross-section. Instead, more of the gas would be dispersed into the downward-moving annular region, causing worse stripping efficiency for the large nozzles. Thus, enlarged nozzles have a negative influence on the stripping efficiency. To maximize stripping efficiency the jet penetration should be close to the radius of the column.

Table 2
Jet penetration lengths predicted by the correlation of Merry (1971) for different diameter nozzles

Nozzle parameters (single nozzle)	Small (3.2 mm)	Normal (6.4 mm)	Large (9.5 mm)
Q_0'	0.0092	0.0092	0.0092
u_0 (m/s)	550	262	92
L_{ave} (m)	0.32	0.25	0.16

All predictions for 97 μm FCC particles of density of 1700 kg/m^3 with air at 25 °C and a pressure of 1.17×10^5 Pa.

In summary, a mega-shed stripper combined with steam injection from spargers, sweeping jets and free jets, achieved stripping efficiencies similar to those for the original commercial design. The mega-shed stripper has potential for commercial cokers, with the likelihood of increasing run length by decreasing fouling, while not increasing total steam utilization.

4. Conclusions

The stripping efficiencies of the +-top, X-bottom mega-shed configuration were somewhat higher than those of the X-top, +-bottom configuration, probably due to different gas–solid flow near the standpipe entrance. Insertion of jet nozzles from the outer wall did not adversely affect the stripping efficiency. Staggered jets near the base of the stripper augmented turbulence, established a dilute region between the two mega-sheds, and improved stripper performance. Spargers can be used to reduce the number of jets when attrition needs are low. Two mega-sheds combined with spargers, sweeping jets and parallel jets showed the highest stripping efficiency of the configurations tested, while combining them only with spargers and sweeping jets also led to stripping efficiencies close to those of the original commercial design with eight rows of shed baffles. Jets sweeping along the tops of the mega-sheds increased stripping efficiencies. Nozzles of increased diameter showed reduced stripping efficiencies, probably due to decreased jet penetration.

Overall, two mega-sheds combined with steam injection via spargers, sweeping jets and free jets provided stripping efficiencies virtually the same as for the original commercial stripper design. Hence the new configuration appears to have potential for commercial application, with the advantage of decreasing both fouling and flooding.

Acknowledgements

The authors are grateful to Syncrude Canada Limited for sponsoring this work and for permission to publish the results. We acknowledge assistance with experiments from Dianle Wang. We also thank Chevron Canada Ltd. for providing the FCC particles.

References

[1] I. Rose, H. Cui, T. Zhang, C. McKnight, J.R. Grace, X.T. Bi, C.J. Lim, Toward an ultimate fluidized stripper, Powder Technol. 158 (1–3) (2005) 124–132.
[2] P. Rivault, C. Ngugen, C. Laguérie, J.R. Bernard, Countercurrent stripper dense circulating beds effect of the baffles, in: J.F. Large, C. Laguérie (Eds.), Fluidization VIII, Engineering Foundation, New York, 1996, pp. 491–499.
[3] R.C. Senior, C.G. Smalley, E. Gbordzoe, Hardware modifications to overcome common operating problems in FCC catalyst strippers, in: L.-S.

Fan, T.M. Knowlton (Eds.), Fluidization IX, Engineering Foundation, New York, 1998, pp. 725–732.

[4] J.M. Matsen, Fluidized beds, in: A. Bisio, R.L. Kabel (Eds.), Scale-up of Chemical Processes, Chapter 10, Wiley Interscience, New York, 1985, pp. 347–405.

[5] B. Knapper, F. Berruti, J.R. Grace, H.T. Bi, C.J. Lim, Hydrodynamic characterization of fluid bed cokers, in: J.R. Grace, J. Zhu, H.I. deLasa (Eds.), Circulating Fluidized Bed Technology VII, CSChE, Ottawa, 2002, pp. 263–270.

[6] H.T. Bi, J.R. Grace, C.J. Lim, D. Rusnell, C. McKnight, Hydrodynamics of the stripper section of fluid cokers, Can. J. Chem. Eng. 83 (2005) 161–168.

[7] X. Song, J.R. Grace, H.T. Bi, C.J. Lim, E. Chan, B. Knapper, C.A. McKnight, Gas mixing in the reactor section of fluid cokers, Ind. Eng. Chem. Res. 44 (2005) 6067–6074.

[8] X.T. Bi, H.P. Cui, J.R. Grace, A. Kern, C.J. Lim, D. Rusnell, X.Q. Song, C. McKnight, Flooding of gas–solids counter-current flow in fluidized beds, Ind. Eng. Chem. Res. 43 (2004) 5611–5619.

[9] L.R. Glicksman, M.R. Hyre, P.A. Farrell, Dynamic similarity in fluidization, Int. J. Multiphase Flow 20S (1994) 331–386.

[10] J.M.D. Merry, Penetration of a horizontal jet into a fluidized bed, Trans. Inst. Chem. Eng. 49 (1971) 189–195.

[11] J.Z. Liu, J.R. Grace, H.T. Bi, A novel multi-functional optical fiber probe, AIChE J. 49 (2003) 1405–1432.

[12] H.P. Cui, M. Strabel, D. Rusnell, X.T. Bi, K. Mansaray, J.R. Grace, C.J. Lim, C.A. McKnight, Gas and solids mixing in a dynamically scaled fluid coker stripper, Chem. Eng. Sci. 61 (2006) 388–396.